INVESTIGATING THE IMPACT OF SOLAR WIND HYDROGEN ON THE MEASUREMENT OF SOLAR WIND MAGNESIUM. E. C. Koeman-Shields[1], G. R. Huss[1], A.J. Westphal[2], R. C. Ogliore[3], A. J. G. Jurewicz[4], D. S. Burnett[5], K. Nagashiima[1], [1]HIGP, University of Hawai'i at Mānoa, 1680 East-West Road, Honolulu, HI 96822 (ekoeman@higp.hawaii.edu), [2]Space Sciences Laboratory, University of California at Berkeley, Berkeley, CA 94720, [3]Dept. of Physics, Washington University in St. Louis, One Brookings Drive, St. Louis, MO 63130, [4]Dept. of Earth Sci., Dartmouth College, Hanover, NH 03755, [5]Div. of Geol. and Planet. Sci., MC 100-23, Caltech, Pasadena, CA 91125.

Introduction: The return of the Genesis mission has allowed for more accurate elemental and isotopic measurements of solar wind [1]. Since working on the Genesis collectors, we have countinuously refined methods for making high-quality SIMS measurements of solar wind. One of the most challenging aspects when measuring the solar wind is standardization. The standard must have the same structure as the solar wind collector. Accordingly, an effective way to standardize a solar wind measurement is to implant a known amount of an isotope standard into the actual Genesis chip (at a different depth than the solar wind) and to measure the solar wind and standard in the same analysis [e.g., 2]. However, the actual Genesis material is inhomogeneous with depth because of the solar wind implant itself. Consequently, it is necessary to understand whether the large hydrogen fluence of the solar wind could have any effect on the measurements of other elements using SIMS. Here we look at Mg: can the amount of H in the solar wind cause any isotope fractionation or alter the sensitivity of SIMS Mg measurements? This study aims to address this possible problem by creating an analog of a Genesis collector with standard implants, with and without H, and measuring them under the same conditions. Magnesium was chosen as the second implant because our group is in the process of collecting an accurate isotopic measurement of Mg in the solar wind using rastered ion imaging [3].

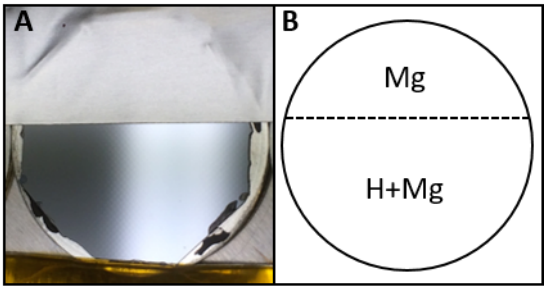

Fig. 1: (A) Si wafer (~1 inch across) with the opaque mask. (B) Schematic of the sample with implant zones shown: ^{24,26}Mg only and ^{1}H with ^{24,26}Mg.

Experimental Methods: A silicon wafer was implanted with ^{1}H, ^{24}Mg, and ^{26}Mg at Kroko, Inc. at fluences similar to Mg/H found in the solar wind. First, an opaque mask was placed over ~1/3 of the wafer and was implanted with ^{1}H at a fluence of $5x10^{16}$ atoms per cm^2 and an energy of 25 keV. The mask was then removed and ^{24}Mg and ^{26}Mg were implanted with a 1:1 ratio at a fluence of $5x10^{12}$ atoms per cm^2 across the wafer's entire surface at energies of 140 KeV and 129 KeV, respectively. These energies are similar to the velocities found in the solar wind. The different implants and mask resulted in the silicon wafer having two implant zones: 1) zone with only ^{24,26}Mg and 2) zone with ^{1}H, and ^{24,26}Mg (Fig. 1).

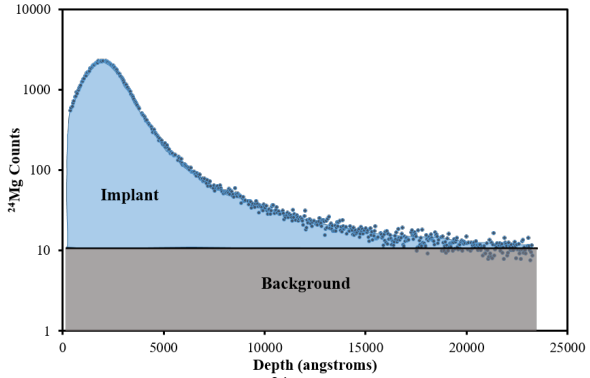

Fig. 2: Depth profile of ^{24}Mg from the area with only the Mg implanted. After integrating the area under the measured profile and that for the background Mg (gray rectangle), the background is subtracted from the total signal to give the integrated value of the implant (blue area).

The Si wafer was measured using the Cameca ims 1280 ion microprobe at the University of Hawai'i at Mānoa. Measurements were made using a focused primary $^{16}O^-$ beam with a beam current of 10 nA in depth-profiling mode. The beam was rastered over a 50 x 50 μm^2 area. A field aperture of 3000 μm was used to exclude the edges of the sputtered crater and to admit the signal from the inner 20 x 20 μm^2 area. After measurements, ion probe pits were imaged using a scanning electron microscope to check for pit anomalies. Pit depths were measured using a MicroXAM interferometer at Dartmouth College. Pit depth measurements by interferometry can depend on both operator focus and surface-oxide thickness; accordingly, each pit was measured several times after stage move-

ment and refocusing. Additionally, the measurements were cross-checked to a silicon reference where the pits were were previously measured using a stylus profilometer calibrated by using step-height standards and also cross-referenced to a similar unit at NIST. The accuracy of the MicroXAM data used here is estimated to be within ~3%.

The first 5 cycles of each measurement were omitted in the data reduction due to Mg contamination on the surface of the Si wafer and the raw counts were normalized to the primary beam current. The background Mg in the Si wafer gives a constant signal that can be well measured below the implant. After integrating the area under the measured profile and that for the background Mg, the background can be subtracted from the total signal to give the integrated value of the implant (Fig. 2). A total of five measurements were completed on the sample, two from the implanted area with both ^{1}H, ^{24}Mg, and ^{26}Mg, and three from the area with only ^{24}Mg and ^{26}Mg implanted. We plan to collect more depth profiles on the sample in the near future to confirm our preliminary findings.

Results and Discussion: In Fig. 3, we show two depth profiles of ^{24}Mg counts from the different implant regions. The depth profile from the area of the sample with both ^{1}H and ^{24,26}Mg implanted measured slightly deeper into the sample when compared to the measurement from the area with just ^{24,26}Mg implanted. This result can be seen in all of the measured depth profiles. A compilation of the integrated background-subtracted totals for ^{24}Mg and ^{26}Mg are summarized in Table 1. The total values of ^{24,26}Mg counts from the implant areas with both H and Mg are higher than those of the areas with only Mg implanted. There is no noticeable systemic effect of the implanted ^{1}H on the ^{26}Mg/^{24}Mg isotope ratio. The averages for the two implant zones have a difference ~0.2‰, while there is a ~5‰ range for the Mg only implant area and a ~4‰ range for the implant area with both H and Mg. A systematic effect of as much as ~8‰ (2σ) cannot be excluded by these measurements. The agreement in our measurements are promising and show much progress; it demonstrates our capability to collect precise data.

These preliminary results indicate that the ^{1}H implant did not cause an isotope fractionation between ^{24}Mg and ^{26}Mg larger than ~8‰. However, the ^{1}H implant appears to be adding to the total counts of ^{24}Mg and ^{26}Mg (Table 1) by about 3%. While more data need to be collected to confirm this effect, the preliminary findings we present here could have an impact on past and future solar wind fluence measurements. If the presence of solar wind H is affecting the SIMS instrumental sensitivity for other elements, then H should be implanted along with the standard implant prior to measurement so one can account for and correct for this effect. H implantation might need to be carried out at several energies and fluences to simulate accurately the actual SW exposure for Genesis. It may also be necessary to carry out experiments to determine whether the relative ordering of H implantation and that of other elements has an effect on the results.

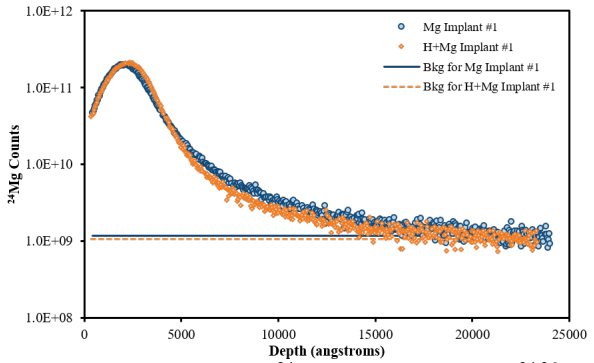

Fig. 3: Depth profiles of ^{24}Mg counts from the ^{24,26}Mg only implant area (blue) and from the implant area with ^{1}H and ^{24,26}Mg (orange), along with their respective backgrounds. Total integration values for these depth profiles can be found in Table 1.

Table 1: Integrated background-subtracted values normalized to primary beam current and ^{26}Mg/^{24}Mg ratios from the two different implant zones.

Measurement	^{24}Mg Counts	^{26}Mg Counts	^{26}Mg/ ^{24}Mg
Mg Implant #1	5.30×10^{14}	5.29×10^{14}	0.9975
Mg Implant #2	5.39×10^{14}	5.35×10^{14}	0.9926
Mg Implant #3	5.44×10^{14}	5.42×10^{14}	0.9969
Average	5.38×10^{14}	5.35×10^{14}	0.9957
H+Mg Implant #1	5.54×10^{14}	5.51×10^{14}	0.9936
H+Mg Implant #2	5.60×10^{14}	5.58×10^{14}	0.9974
Average	5.57×10^{14}	5.54×10^{14}	0.9955

References: [1] Burnett, D. S. (2013) MAPS 48, 2351-2370 [2] Koeman-Shields, E. C. et al. (2016) *LPSC XLVII*, Abstract #2800. [3] Westphal, A. J. (2014) *LPSC XLV,* Abstract #2671. Supported by NASA Grant NNS14AF25G to GRH.